

IMPACT OF ELECTROSTATIC PERTURBATIONS ON PROXIMITY OPERATIONS IN HIGH EARTH ORBITS

Kieran Wilson* and Hanspeter Schaub†

Orbital rendezvous is a highly challenging operation conducted in space, but is required for a range of missions. While low Earth orbit rendezvous has become routine with vehicles ferrying astronauts and cargo to the International Space Station, a range of missions propose to rendezvous in near-Geostationary orbit. This region is known to experience high levels of electrostatic charging, which can result in perturbing intercraft forces and torques during proximity operations. A range of proximity operations that model a servicing mission with a non-functional target are modeled to evaluate the impact of electrostatic perturbations, including rendezvous trajectories and static holds. Perturbing electrostatic torques are evaluated using the multi-sphere method and result in the target body rotating, requiring the servicer to maintain its relative position by translation. Electrostatic perturbations induced by potential magnitudes that have been observed at high earth orbits are found to be significant. Following a nominal rendezvous trajectory with 10 kV on each spacecraft results in the target rotating over 280° at up to $0.1^\circ/\text{s}$ prior to docking, while a 5 hour hold at 10 meters separation under the same conditions can result in 100-fold increase in control effort over an unperturbed case, and can be even larger depending on the relative positions of the servicer and target.

MOTIVATION AND INTRODUCTION

After decades of planning, orbital servicing is finally moving from a promising, albeit futuristic, concept to near-term reality. The Mission Extension Vehicle (MEV-1) from Northrup Grumman's SpaceLogistics subsidiary launched in mid October of 2019, as the first commercial satellite servicing mission. MEV-1 successfully rendezvoused with Intelsat 901 in the geostationary orbit (GEO) graveyard, physically latching onto Intelsat 901 and assuming station keeping and attitude control responsibilities for the fuel-depleted communications satellite. This effectively adds years of useful life to the otherwise functional communications satellite [1]. Similarly, NASA is planning a robotic refueling demonstration of the Landsat 7 spacecraft, a vehicle which was never designed for servicing, within 3 years [2]. These missions, and a range of related concepts for orbital operations, illustrate a rapid maturation of robotic servicing technologies, all of which are dependent on automated rendezvous operations.

In a related field, the need for active debris removal (ADR) in all orbital regimes is becoming more pressing with every collision and near miss. The addition of tens of thousands of spacecraft as mega-constellations become established will only further heighten the need to begin removal of potentially hazardous debris objects [3]. Such operations, whether for servicing or debris mitigation,

*Graduate Research Assistant, Ann and H.J. Smead Aerospace Engineering Sciences Department, University of Colorado Boulder, 80301

†Glenn L. Murphy Endowed Chair, AIAA and AAS Fellow, Ann and H.J. Smead Aerospace Engineering Sciences Department, University of Colorado Boulder, 80301

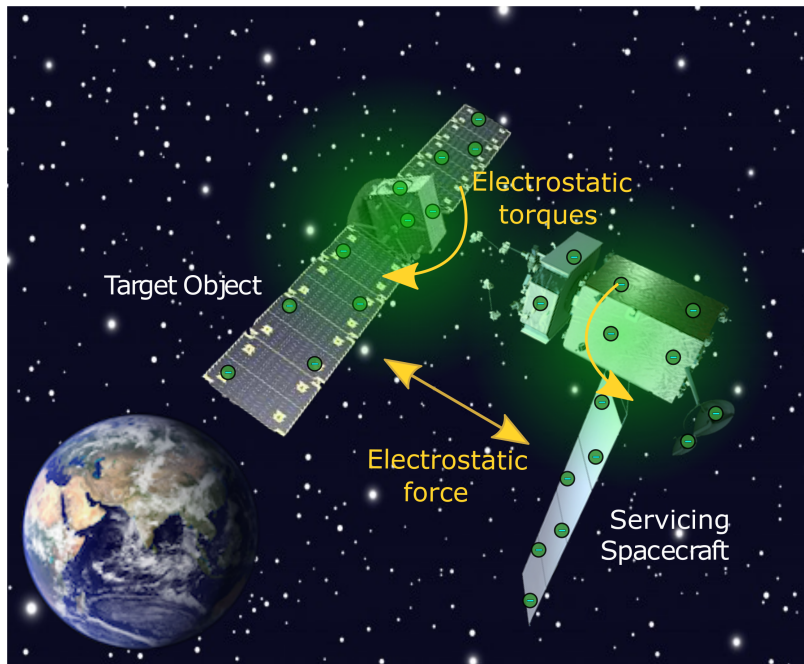


Figure 1: Concept figure of a high Earth orbit servicing mission perturbed by electrostatic forces and torques.

will inevitably require automated rendezvous. However, few servicing operations have ever been conducted on orbit (space stations such as the ISS and Mir, as well as the Hubble Space Telescope are notable exceptions), and none other than MEV-1 have occurred in GEO. Additionally, all of these rendezvous maneuvers occurred with well characterized, cooperative targets, which cannot be assumed for a debris remediation or repair mission.

Spacecraft develop electrostatic charges through interactions with the space environment, where currents arise through solar-induced photoelectric electron emission, bombardment by plasma ions and electrons, and the backscattered and secondary electron emissions that result from those impacts [4]. While spacecraft charging can occur in low earth orbit, particularly in orbits that cross the auroral regions, these events are typically limited to kV levels and are relatively fleeting [5]. However, beyond LEO, environmental plasma parameters become more conducive to heightened and sustained spacecraft charging; the ATS-6 mission recorded potentials as high as -19 kV [6]. Additionally, the increasing Debye length that comes with sparser, more energetic plasmas at higher altitudes results in less shielding of electrostatic charges and therefore greater electrostatic interactions between spacecraft operating in close proximity. In GEO regions, for instance, Debye lengths are typically on the order of 100 meters, compared with centimeters at LEO [7].

A significant body of prior work has focused on the use of controlled spacecraft charging to achieve desired intercraft forces and torques. These concepts cover using electrostatic forces for propellant-less Coulomb formation flying, as introduced by references [8, 9], as well as related concepts like the Electrostatic Tractor for active debris detumbling and re-orbiting in GEO, introduced in reference [10], and with reference [11] providing a recent survey of work in the field. However, relatively little work has focused on the impacts of natural charging on spacecraft relative motion, though reference [8] found that significant torques could be generated by intercraft electrostatic

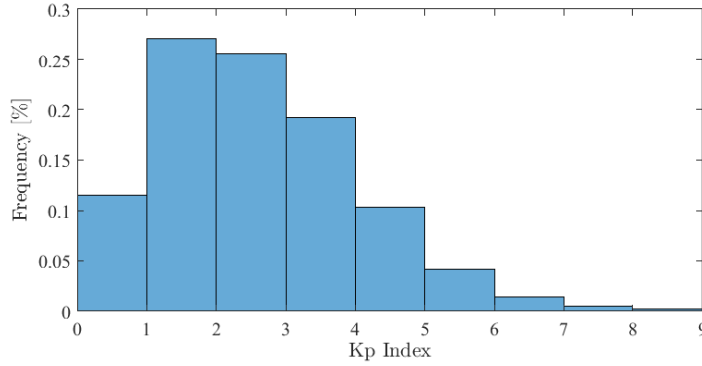


Figure 2: Distribution of Kp index values over the last 4 solar cycles (October 1964-December 2019).

forces as a result of natural charging. With increasing interest in rendezvous in high altitude orbits prone to charging—from GEO to cislunar space—it will become necessary to assess the impact of charging on rendezvous dynamics to ensure mission success.

This work analyzes the impact of charged spacecraft on the dynamics of proximity operations between an active spacecraft and an inert or disabled target object. This paper is organized as follows: first, the general frequency of spacecraft charging in high earth orbits is discussed for context. Then a method to rapidly evaluate electrostatic forces and torques is discussed, followed by the use of that technique in developing a 6DOF, 2-craft simulation of a controlled servicer and an inert target vehicle. Results from simulations with different spacecraft geometries for both rendezvous trajectories and static holds are discussed.

FREQUENCY OF CHARGING

Spacecraft charging in the GEO region is known to occur more frequently during enhanced electron fluxes associated with geomagnetic storm time conditions. The global K_p index, is a widely used measure of geomagnetic disturbance, evaluated every 3 hours on a 0-9 scale with higher values indicating a more disturbed magnetic field. Data for the K_p index every 3 hours for the last 5 solar cycles, spanning October 1964 to December 2019, was obtained from Reference [12]. For the majority of measurements over the last 4 solar cycles, the K_p index was at a value of 2 or lower as seen in Figure 2, indicating relatively quiet geomagnetic conditions. However, 26% of measurements recorded $K_p=3$ or higher, indicating a somewhat disturbed geomagnetic environment, with approximately 4% of measurements exceeding $K_p=4$, indicating a storm condition. These events are concentrated around periods of solar maximum, and a 30-day sliding window applied to the data reveals some 30 day periods with over 31% of measurements at $K_p > 4$.

Charging events can still occur during periods of quiet ($K_p < 3$), but tend to be less likely, less intense and less prolonged [13]. Reference [13] found that times of elevated K_p were associated with a 30% chance of experiencing charging events, compared with low single-digit probabilities during low K_p periods. Ultimately, this suggests that, while severe electrostatic charging that could result in significant perturbations during proximity operations are rare, periods with frequent charging events can occur, warranting further consideration of the impacts of electrostatic charging on proximity operations.

COMPUTING ELECTROSTATIC FORCES AND TORQUES

The electrostatic force for the simplest case between two point charges can be found as Coulomb's law, proportional to the product of the charge magnitudes (q_1 and q_2), and inversely proportional to the square of the distance between the charges (r) as

$$F_c = K_c \frac{q_1 q_2}{r^2} \quad (1)$$

where K_C is Coulomb's constant, defined as $K_C = 1/4\pi\epsilon_0 \approx 8.99 \times 10^9 \text{ Nm}^2/\text{C}^2$.

The charge q of a physical object is related to the capacitance, C , by the voltage, V :

$$q = VC \quad (2)$$

Therefore, if the voltage of an object is known, then the capacitance can be used to determine charge, which can then be used to determine the force acting between two bodies. However, objects in close proximity will exhibit mutual capacitance effects, which must be accounted for to accurately determine the total charge on each object. For the simplest 3D case with two spheres in a pure vacuum, the potentials (V_A and V_B) can be used to determine the total charge on each sphere using the relation [14]

$$\begin{bmatrix} q_1 \\ q_2 \end{bmatrix} = \underbrace{\frac{d}{k_c(d^2 - R_1 R_2)} \begin{bmatrix} dR_1 & -R_1 R_2 \\ -R_1 R_2 & dR_2 \end{bmatrix}}_{C_V} \begin{bmatrix} V_1 \\ V_2 \end{bmatrix}. \quad (3)$$

where d is the distance between each sphere center, and R_1, R_2 are the sphere radii.

If the capacitance of a spacecraft is known, then it can be approximated as a sphere with a radius that results in an equivalent capacitance. The capacitance of a sphere is given by the analytical expression:

$$C_{\text{sphere}} = 4\pi\epsilon_0 R. \quad (4)$$

However, two spheres only roughly approximate the electrostatic forces between two spacecraft, and fail to capture any of the torques associated with the bodies; these limitations can be overcome with the use of multiple spheres. The Multi-Sphere Method (MSM) quickly and accurately approximates the distribution of electric charge on a body through the use of a series of spheres [15]. Given the potential on each sphere and its location relative to all other spheres, it is possible to analytically compute the charge on each sphere:

$$\begin{pmatrix} V_1 \\ V_2 \\ \vdots \\ V_n \end{pmatrix} = k_c \begin{bmatrix} 1/R_1 & 1/r_{1,2} & \dots & 1/r_{1,n} \\ 1/r_{2,1} & 1/R_2 & \dots & 1/r_{2,n} \\ \vdots & \vdots & \ddots & \vdots \\ 1/r_{n,1} & 1/r_{n,2} & \dots & 1/R_n \end{bmatrix} \begin{pmatrix} Q_1 \\ Q_2 \\ \vdots \\ Q_n \end{pmatrix}, \quad \mathbf{V} = [S]\mathbf{Q} \quad (5)$$

Here $[S]$ denotes the elastance matrix, which is also the inverse of the capacitance matrix.

The total force acting on body 1, composed of charges q_j , can be found by summing the forces of each sphere in body 2 (charges q_i) on each sphere in body 1:

$$\mathbf{F} = k_c \sum_{j=1}^{n_1} q_j \left(\sum_{i=1}^{n_2} \frac{q_i}{r_{i,j}^3} \mathbf{r}_{i,j} \right) \quad (6)$$

With the force between each pair of charges known, this formulation can be easily extended to find the torque acting on each body:

$$L_O = k_c \sum_{j=1}^{n_1} q_j \left(\sum_{i=1}^n \frac{q_i}{r_{i,j}}^3 \mathbf{r}_i \times \mathbf{r}_{i,j} \right) \quad (7)$$

The MSM method is predicated on the knowledge of some property of the target body, whether charge, capacitance or electric field [14]; at that point an arbitrary number of spheres can be placed and their radii adjusted to match the desired property of the MSM model to the truth value. Increasing the number of spheres improves the accuracy of the model, but at increased computational cost. Capacitance is a function of the object’s geometry and is therefore the property used here. Analytic solutions for the capacitance of an object are available for only a select few shape primitives (such as spheres or infinite wires). Therefore, a finite element scheme must be used to find the capacitance of the spacecraft, which can then be used to establish a MSM model that is fast enough for computations.

The Method of Moments (MOM) is a finite element method which can be used to determine the capacitance of an arbitrary shape. The shape is first discretized into a triangular mesh, and the capacitance of each triangular area calculated. Then, the mutual capacitance effects of all other triangular areas in the body on the initial triangle are computed. Repeating this process for each element allows the elastance matrix for the object to be computed [16].

While a significant body of work had explored variations of the multisphere method, including references [16, 17, 14, 18], this work involved the overall MSM model changing significantly with time, as the two spacecraft approached from tens of meters to tens of centimeters. The MSM formulation has been validated for time-varying shapes and structures in [15]. The results of that work means that the true capacitance of each spacecraft only needs to be computed once, and the MSM model tuned from that truth capacitance is valid across a wide range of conditions.

For the case with two interacting bodies, the elastance matrix $[S]$ can be written in block form as

$$\begin{bmatrix} V_1 \\ V_2 \end{bmatrix} = \begin{bmatrix} S_1 & S_M \\ S_M^T & S_2 \end{bmatrix} \begin{bmatrix} Q_1 \\ Q_2 \end{bmatrix} \quad (8)$$

where the S_M terms refer to the mutual capacitances, the components which vary with the relative positions of the two bodies. Only the mutual capacitances need to be updated at each timestep as the spacecraft move relative to each other, so the MSM sphere radii and the self-capacitance matrices S_1 and S_2 do not need to be recomputed, which saves significant computational effort.

It is important to note that the structures considered here are assumed to be continuously conducting, as is recommended in design guidelines for mitigating electrostatic charging. However, if the structure were not fully conducting, sections of the spacecraft could develop significantly different potentials, with differential charging resulting in several kV differences across the spacecraft [19].

MODEL AND SCENARIO SETUP

Spacecraft Models

The scenario considered here involves a servicer (based on the Northrup Grumman MEV-1 GEO servicing vehicle) rendezvousing with an uncooperative target. One of NOAA’s next-generation

GOES spacecraft (the GOES-R) was chosen as an example target; these craft are crucial for weather forecasting in space and on earth, and cost over \$2.5 billion each [20]. They also operate on traditional chemical propellants, so it is reasonable that NOAA may want to service or refuel them in the future to extend their service lives.

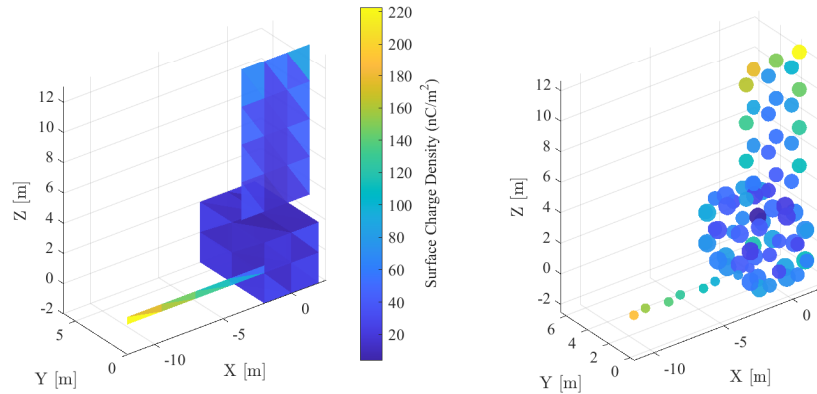


Figure 3: The GOES-R spacecraft approximated as a method of moments finite element model (left) and an 80-sphere MSM model (right).

Publicly available photographs and published dimensions of each craft were used to construct MoM models, with an example GOES-R spacecraft model shown in Figure 3 [20]. However, inertia properties are rarely published, and knowledge of the center of mass and the inertia matrix of the uncontrolled target are necessary to accurately model the impact of electrostatic forces and torques. Therefore, these properties had to be estimated.

A CAD model of the GOES-R spacecraft was developed in Solidworks, using approximate vehicle and fuel tank dimensions from Reference [20]. Published fueled and dry masses were used to determine the mass of fuel on board, which could then be modeled as evenly distributed through each tank volume. The remaining dry mass was assumed to be evenly distributed through the spacecraft, excluding the tanks. This model could then be used to calculate inertia properties and center of mass locations. While approximate, these numbers reflect a reasonable starting point for this analysis, where the goal is not to determine how a *specific* object will respond to electrostatic forces and torques, but instead to evaluate the *general impact* of these perturbations. For this end of life servicing mission, the fuel tanks were assumed to be empty and the resultant mass properties used.

Dynamics

The perturbations of interest occur over small separation distances, on the order of tens of meters, which a rendezvousing spacecraft is required to traverse during final approach. Additionally, these effects are predominant in regions of high spacecraft charging, such as GEO. The combination of very close formation flight (tens of meters), large orbital radii with small eccentricities (a over 42000 km, $e = 0.0001$) and relatively short time periods makes the dynamics well suited to linearization,

so Hill-Clohessey-Whiltshire (HCW) equations of relative motion in equation 9 are used [21].

$$\begin{aligned}\ddot{x} &= 3n^2x + 2n\dot{y} + a_x \\ \ddot{y} &= -2n\dot{x} + a_y \\ \ddot{z} &= -n^2z + a_z\end{aligned}\tag{9}$$

Two spacecraft are established as deputies relative to a virtual Keplerian chief orbiting in a GEO graveyard. The deputies exert mutual forces and torques due to electrostatic interactions, so they will exhibit perturbed motion relative to the Keplerian chief frame \mathcal{H} . The first deputy, which represents the uncontrolled target for rendezvous, is initially located at the origin of the HCW frame, while the second spacecraft (the controlled servicer) is set at an initial position determined by the scenario under consideration.

Translational dynamics constitute only one part of the problem, however. The two spacecraft exert mutual torques on each other which will perturb their attitudes. The torques (L) acting on each craft can be related to the angular rotational rate of each body (ω) by the equation of motion

$$[I]\dot{\omega} = -\tilde{\omega}[I]\omega + L\tag{10}$$

where the tilde represents the skew symmetric matrix operator, and $[I]$ represents the inertia tensor [21]. Quaternions are used to represent attitudes, and the attitude of the servicer was prescribed to match the attitude of the target at each time step to simulate active relative attitude control of the servicer relative to the target object.

At each time step the translational states and rates are integrated using the CW equations, while Euler's equation of rotational motion is used to integrate rotational rates and the quaternion differential equation of motion is used to integrate attitude states.

Reference trajectory

There are four relevant reference frames for this scenario: \mathcal{N} -an earth-centered inertial frame, \mathcal{H} - an unperturbed co-orbiting origin point for the Hill-frame, \mathcal{T} -a body-fixed frame on the target spacecraft, with an origin at the docking point, \mathcal{S} - a body-fixed frame at the docking point on the servicer.

The reference trajectory is defined in frame \mathcal{T} fixed to the docking point on the target, as would be expected for a servicing scenario, and is shown in Figure 4. As the target spacecraft rotates due to perturbing torques, the reference trajectory is also rotated in the HCW frame. The trajectory is based on public videos of the MEV-1 final trajectory; the servicer begins 80 meters from the target, and follows a straight trajectory to the interface point. Several holds are built in along the way, with 10 minutes each at 20 meters, 10 meters and 3 meters from the target. The terminal point is 1 meter from the docking location, at which point physical grasping mechanisms take over during a final 30 minute hold.

A pre-computed reference trajectory (shown in Figure 4) is used here, and the controller tracks the reference as it evolves with time. The inherently coupled dynamics of the two spacecraft can increase the risk of collision as induced torques on the target spacecraft can result in collisions between antennas or arrays on the target and the servicer. In these cases it may only take a few degrees of target rotation to cause contact with the servicer.

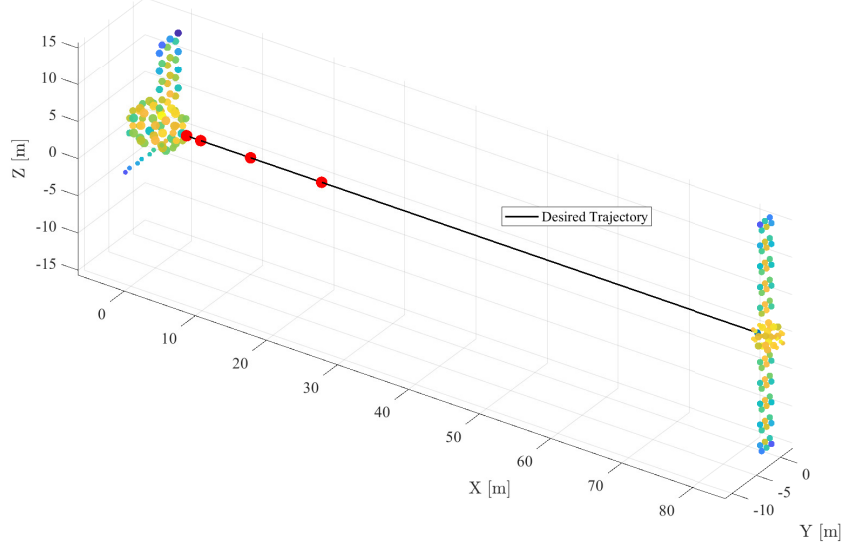


Figure 4: The reference trajectory from the servicer (right) to the disabled target (left). The hold points are shown as red dots.

Controller

A Lyapunov-derived reference tracking controller was implemented to follow a desired trajectory, computing the desired control authority as[21]

$$\mathbf{u} = -(\mathbf{f}(\mathbf{r}_d) - \mathbf{f}(\mathbf{r}_{d_d})) - [K_1] \Delta \mathbf{r} - [K_2] \Delta \dot{\mathbf{r}} \quad (11)$$

where $\Delta \mathbf{r}$ represents the difference between the spacecraft actual position and desired position in the target's reference frame, and $\Delta \dot{\mathbf{r}}$ represents the velocity difference in the same frame. The term $(\mathbf{f}(\mathbf{r}_d) - \mathbf{f}(\mathbf{r}_{d_d}))$ represents the relative inertial acceleration between the vehicle and the target orbit, evaluated numerically at each timestep. To mimic a servicer case where the spacecraft potentials are unknown, this relative acceleration term includes only relative accelerations due to gravity, not the electrostatic perturbations. The gain matrices $[K_1]$ and $[K_2]$ were manually tuned to achieve desired performance.

The goal of this work is to evaluate the contribution of a specific perturbation (electrostatics), so navigational or controller noise were not included, and perfect knowledge of relative states assumed. However, the control authority was limited to account for thruster saturation effects. For the MEV-1 mission, final approach and rendezvous control was provided by a mix of 1-Newton and 22-Newton hydrazine thrusters developed by Aerojet Rocketdyne; given a spacecraft mass of approximately 2300 kg, the 22N thrusters set an upper acceleration limit of $\sim 0.01 \text{ m/s}^2$ which was used here [22]. The servicer's attitude was prescribed to match the attitude of the target, ensuring docking faces remained aligned.

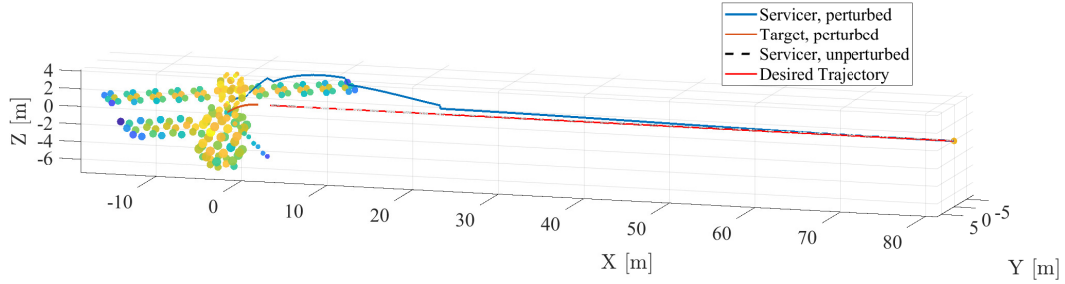


Figure 5: The rendezvous trajectory with a 7kV potential on each craft.

RESULTS

All cases here are evaluated with equal charges on each spacecraft. As both spacecraft are exposed to near-identical environmental conditions (assuming one is not shadowing the other), it is reasonable to assume that each has a similar potential, though there may be some difference due to variations in design or material properties. As discussed earlier, the spacecraft are considered to be fully conducting, though this assumption may need to be reconsidered depending on the specific target vehicle.

The results are organized as follows: first, the case of a nominal rendezvous is considered, and the impact of electrostatic charging on this trajectory evaluated. The more general case of a servicer maintaining a static position relative to the target is then evaluated, and the impact of different spacecraft geometries, relative positions and potentials assessed.

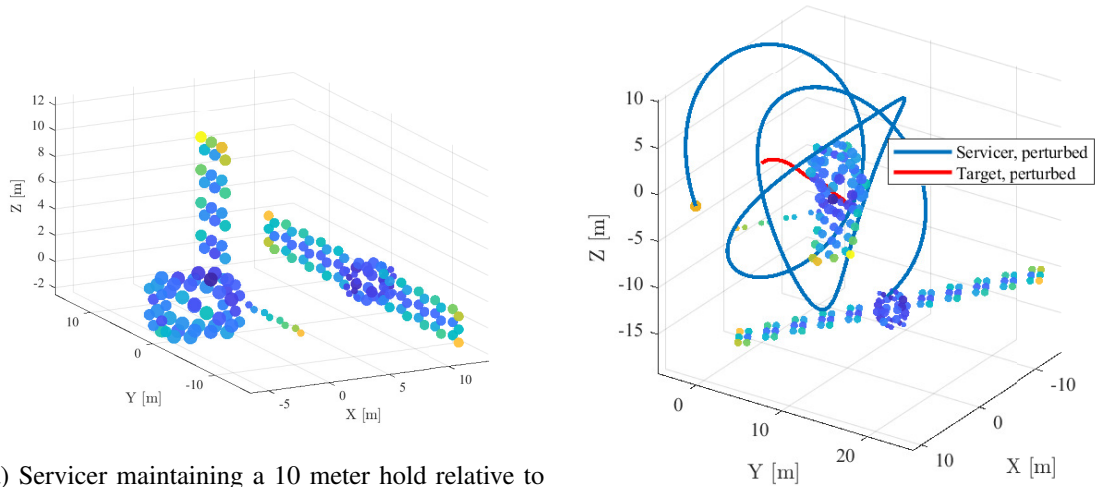
Nominal rendezvous

For a case where the spacecraft are both charged to 7 kV, the torques result in the target reaching rotational rates of 0.03 deg/s and traveling over 100 degrees by the end of the rendezvous. The servicer has to maneuver to track the reference trajectory, which is rotating with the target as seen in Figure 5; this results in a 25% increase in ΔV over the course of the maneuver.

The significance of these perturbations increases as the charge magnitude increases. At 20 kV potentials, rotation rates reach over 0.5 deg/s, and ΔV is over five times what it was for the unperturbed case. This perturbation could be significant even during maneuvers with zero desired relative motion, such as a station keeping hold, with a 10 meter hold requiring over 20 times more fuel for a 7 kV potential case than a 0V one.

Static hold evaluation

To gain further insight into the impact of electrostatic perturbations on proximity operations, a case where the servicer holds a fixed position relative to the target is considered. In this case, the servicer maintains a position 10 meters from the target in the Hill-frame \hat{x} direction. Figure 6b shows the trajectory followed by the servicer over this period to maintain a fixed position at $[10, 0, 0]$ meters in the target frame. As with the rendezvous scenario, the target is initialized with no rotational motion, but is considered to be inert, and therefore affected by electrostatic perturbations. Each hold was evaluated over an arbitrary 5 hour period.



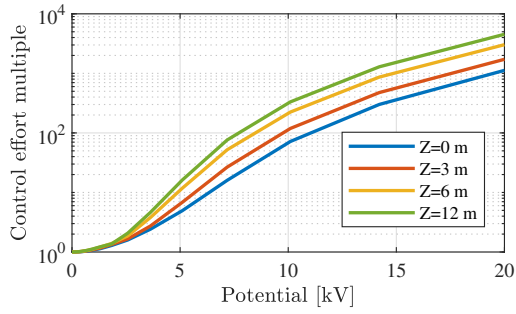
(a) Servicer maintaining a 10 meter hold relative to the target, both craft at 0 kV.

(b) Servicer maintaining a 10 meter hold relative to the target for 5 hours, both craft at 10 kV.

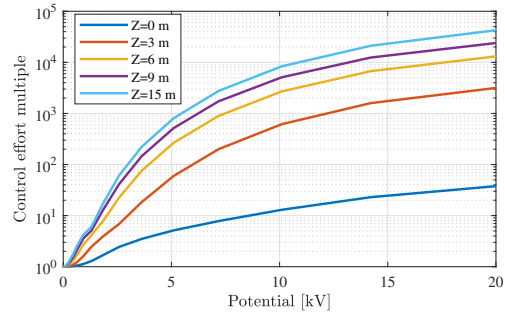
Figure 6: Results of servicer holding a fixed position relative to a target for a 5 hour hold, shown in the Hill frame. Electrostatic torques result in a significant tumble being imparted to the target, despite it having no initial rotation.

To quantify the increase in control effort caused by the electrostatic perturbations for the hold case with an asymmetric GOES-R target, a sweep of parameters was run. These simulations used the same x-offset for the hold point in the target frame, but varied the \hat{z} position, from the target spacecraft docking location up to the top of the target’s solar array. This allows the impact of relative position on control effort to be evaluated, as moving the servicer center of charge further from the center of mass of the target will result in larger effective torques. This trend can be seen in the resulting control effort increase seen in Figure 7b. Even when the servicer is aligned with the target’s docking port at $z = 0$ meters, the torques generated by 10 kV potentials result in a control effort increase of over $90\times$ the unperturbed case, while a hold level with the top of the solar array yields an increase of over $200\times$ the unperturbed case. Additionally, the maximum acceleration required by the servicer to maintain a position 10 meters away from the target at 10 kV was approximately 1 mm/s^2 , which could saturate the 1 N thrusters used as part of the fine maneuvering system on MEV-1 [22]. These numbers are illustrative of the impact of a specific combination of charging and spacecraft geometries, and the large control effort multiple is, in part, a function of the very low ΔV required to maintain a fixed relative position over a few hours at GEO with no initial errors. However, these numbers demonstrate that proximity operations can be significantly perturbed by electrostatic interactions.

While it is expected that the case of an asymmetrical target like the GOES-R spacecraft would experience significant electrostatic torques, it is possible for symmetric targets to experience these perturbations as well. More generally, any case where the electrostatic force vector is not co-linear with the vector from the servicer center of charge (CoC) to the target center of mass (CoM) will result in a net torque on the target. Due to mutual elastance effects, as one charged body approaches another the center of charge location of each body will change. Figure 8b shows how the Z-position

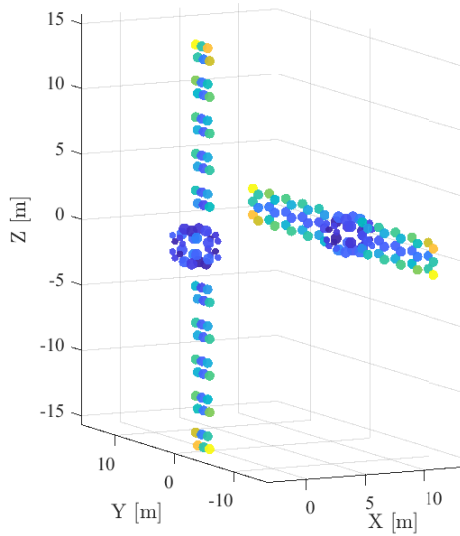


(a) Control effort multiple with asymmetric GOES-R target.

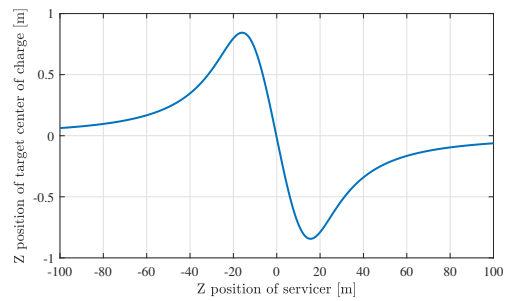


(b) Control effort multiple with symmetric SSL-1300 target.

Figure 7: Increase in control effort (as a multiple of the ΔV for the 0V case) required to hold a fixed 10 meter offset from the target for different servicer \hat{z} positions.



(a) Initial position of servicer and target used for parameter sweeps. Target is centered at the origin, servicer is offset by 10 m in the X direction.



(b) Change in Center of Charge (CoC) position of the target as a function of servicer location.

Figure 8: Variation in target parameters with changing servicer position.

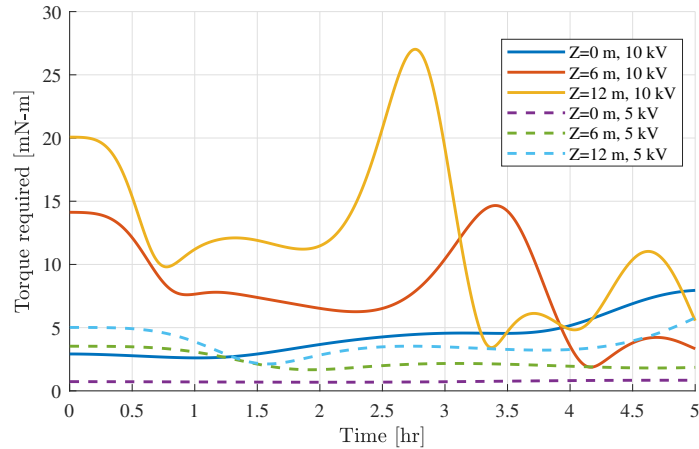


Figure 9: Torque required by servicer to maintain a relative orientation to the target

of the center of charge of a symmetrical spacecraft is impacted by the relative position of a nearby object. For this case, where both craft were held at 10 kV potentials, the center of charge position is shifted by up to ± 85 cm by induced capacitance effects of the nearby servicer.

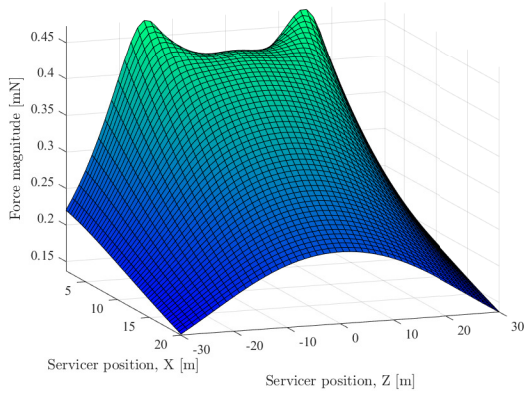
Servicer attitude control requirements

As the target tumbles, the servicer must both translate and rotate in order to maintain a fixed relative orientation. The attitude of the servicer is prescribed to match that of the target in this scenario, but the torque required can be computed at each timestep by rearranging equation 10.

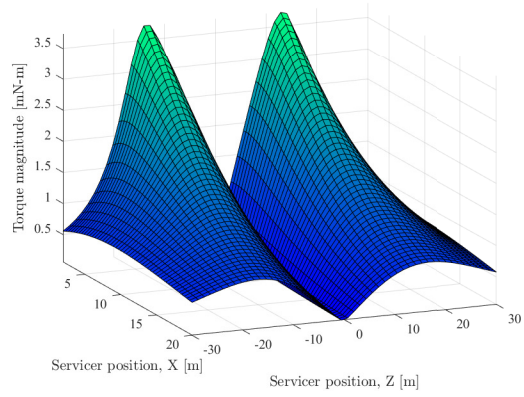
The inertia matrix was taken to be the same as the one estimated for the GOES-R spacecraft, as an estimate for a generic large GEO spacecraft. Figure 9 shows the torque required for the servicer to maintain its orientation relative to the target during the hold at different Z positions and potentials. As would be expected, increasing the Z offset away from the target spacecraft centerline results in higher torque requirements for the servicer, as does increasing the potential of the spacecraft from 5 kV to 10 kV. In both cases, these changes increase the torque acting on the target, so it is logical for the servicer to then require higher torque levels to maintain relative attitude. The highest required torque, for the $Z = 12\text{m}$ and 10 kV potential case, is over 27 mN-m. Large reaction wheels, such as the Honeywell HR-12, are capable of generating torques of 100-200 mN-m, suggesting that these torques are achievable but significant [23]. The accumulated momentum in the reaction wheels as a result of these attitude maneuvers could present another limiting factor in control during charged proximity operations.

A plot like those in Figures 10b and 11b can be used to evaluate trajectories that are likely to impart significant undesired torques to the target body. In the case with two symmetrical spacecraft in Figure 10b, an approach that aligns the center of charge with the center of mass for the target results in minimal torques (the valley along $z = 0$), while approaches near the ends of the solar arrays will impart the most significant torques (the peaks).

However, while it is possible to find low-torque trajectories in the case of a symmetric target spacecraft, for an asymmetric vehicle like the GOES-R there is no path which will not impart torques on the target, as seen in Figure 11b. Many real-world spacecraft will likewise have asymmetric pro-

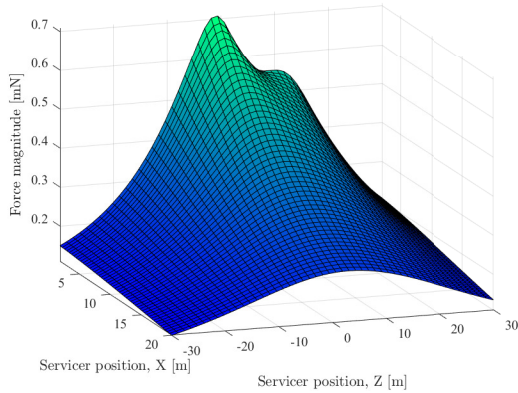


(a) Force on target for different servicer positions.

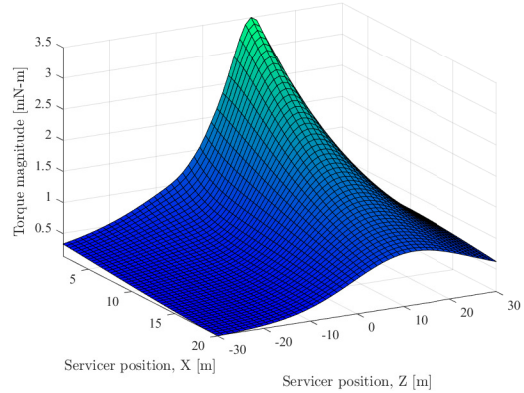


(b) Torque magnitude acting on target as a function of servicer position.

Figure 10: Force and torque for different servicer positions. All evaluated at 10 kV, with both spacecraft using the symmetric two-panel MSM models.



(a) Force on GOES-R target for different servicer positions.



(b) Torque magnitude acting on GOES-R target as a function of servicer position.

Figure 11: Force and torque for different servicer positions. All evaluated at 10 kV, with a servicer based on the symmetric two-panel MSM model, and a target based on the GOES-R model.

trusions, whether solar arrays or communications antennas. Some GEO communications satellites have very large antennas or reflectors; the primary reflector on Echostar T1 is 18 meters in diameter and offset to one side of the spacecraft bus [].

As a point of comparison for the significance of the electrostatic forces and torques, a first order estimate of the worst-case magnitude of solar radiation pressure-induced torque was carried out. Using the maximum projected area of the spacecraft (approximately 24 m^2 and assuming directly incident sunlight on a perfectly reflecting surface, the SRP-induced torque is found to be approximately 0.5 mN-m in the worst case, and quickly decreasing if the orientation of the spacecraft is not aligned with the sun vector, or if it is not perfectly reflecting. This torque is about an order of magnitude below the worst-case electrostatic torque, and the worst-case SRP force ($\sim 0.1 \text{ mN}$)

is about a factor of 5 below the the worst-case electrostatic force. Additionally, while SRP falls off as the face rotates away from the sun, the electrostatic torques will continue to be exerted as long as the servicer is maintaining a relative position, continuing the rotational acceleration of the target. Therefore, the electrostatic perturbations acting on the target are likely to be the dominant disturbance at GEO during periods of significant spacecraft charging.

CONCLUSIONS

Ultimately, these results demonstrate that charging conditions which have been observed at GEO present significant perturbations to proximity operations, and should be modeled in rendezvous and proximity operations development. Perturbing torques between modeled spacecraft at 10 kV are shown to be an order of magnitude larger than SRP, and can dramatically increase the control effort required to perform proximity operations.

For some cases, such as a servicer which must inspect or repair a solar array, or a significantly asymmetric target object, it will be impossible to completely avoid imparting disturbing torques to the target. However, changing the attitude of the servicer on approach, or altering solar array orientations, may help in minimizing these torques. Developing control and guidance strategies to feedforward on estimates of electrostatic potentials on each spacecraft to improve proximity operations perturbed by charging will be a goal of future work.

REFERENCES

- [1] S. Clark, "Two commercial satellites link up in space for first time," *SpaceFlight Now*, 2020.
- [2] B. B. Reed, R. C. Smith, B. J. Naasz, J. F. Pellegrino, and C. E. Bacon, *The Restore-L Servicing Mission*, 10.2514/6.2016-5478.
- [3] Y. S. Karavaev, R. M. Kopyatkevich, M. N. Mishina, G. S. Mishin, P. G. Papishev, and P. N. Shaburov, "The dynamic properties of rotation and optical characteristics of space debris at geostationary orbit," *Advances in the Astronautical Sciences*, Vol. 119, 2004.
- [4] S. T. Lai, *Fundamentals of Spacecraft Charging: Spacecraft Interactions with Space Plasmas*. Princeton University Press, 2011.
- [5] P. C. Anderson, "Characteristics of spacecraft charging in low Earth orbit," *J. Geophys. Res.*, Vol. 117, 07 2012, p. A07308, 10.1029/2011JA016875.
- [6] R. Olsen, "The record charging events of ATS-6," *Journal of Spacecraft and Rockets*, Vol. 24, 1987.
- [7] C. R. Seubert, L. A. Stiles, and H. Schaub, "Effective Coulomb Force Modeling For Spacecraft In Earth Orbit Plasmas," *Advances in Space Research*, 2014.
- [8] L. B. King, G. G. Parker, S. Deshmukh, and J.-H. Chong, "Spacecraft Formation-Flying using Inter-Vehicle Coulomb Forces," tech. rep., NASA/NIAC, January 2002.
- [9] L. B. King, G. G. Parker, S. Deshmukh, and J.-H. Chong, "Study of Interspacecraft Coulomb Forces and Implications for Formation Flying," *AIAA Journal of Propulsion and Power*, Vol. 19, May–June 2003, pp. 497–505.
- [10] H. Schaub and D. F. Moorer, "Geosynchronous Large Debris Reorbiter: Challenges and Prospects," *The Journal of the Astronautical Sciences*, Vol. 59, No. 1–2, 2014, pp. 161–176.
- [11] M. Bengtson, K. Wilson, J. Hughes, and H. Schaub, "Survey of the electrostatic tractor research for reorbiting passive GEO space objects," *Astrodynamics*, Vol. 2, No. 4, 2018, pp. 291–305.
- [12] M. S. T. K. M. Nose, T. Iyemori, "Kp Index," World Data Center for Geomagnetism, Kyoto, 2020, 10.17593/15031-54800.
- [13] A. Ozkul, A. Lopatin, and A. Shipp, "INITIAL CORRELATION RESULTS OF CHARGE SENSOR DATA FROM SIX INTELSAT VIII CLASS SATELLITES WITH OTHER SPACE AND GROUND BASED MEASUREMENTS," 2004.
- [14] D. Stevenson and H. Schaub, "Multi-Sphere Method for Modeling Electrostatic Forces and Torques," *Advances in Space Research*, Vol. 51, Jan. 2013, pp. 10–20, 10.1016/j.asr.2012.08.014.
- [15] J. Maxwell, K. Wilson, J. Hughes, and H. Schaub, "Multisphere Method for Flexible Conducting Space Objects: Modeling and Experiments," *AIAA Journal of Spacecraft and Rockets*, Vol. 57, No. 2, 2020, pp. 225–234, 10.2514/1.A34560.

- [16] J. A. Hughes and H. Schaub, "Heterogeneous Surface Multisphere Models Using Method of Moments Foundations," *Journal of Spacecraft and Rockets*, Vol. 56, No. 4, 2019, pp. 1259–1266, 10.2514/1.A34434.
- [17] H. Engwerda, "Remote Sensing for Spatial Electrostatic Characterization using the Multi-Sphere Method," Master's thesis, Delft University of Technology, Delft, The Netherlands, March 2017.
- [18] P. Chow, J. Hughes, T. Bennett, and H. Schaub, "Automated Sphere Geometry Optimization For The Volume Multi-Sphere Method," *AAS/AIAA Spaceflight Mechanics Meeting*, Feb. 14–18 2016.
- [19] R. C. Olsen, C. E. McIlwain, and E. C. Whipple Jr., "Observations of differential charging effects on ATS 6," *Journal of Geophysical Research: Space Physics*, Vol. 86, No. A8, 1981, pp. 6809–6819, 10.1029/JA086iA08p06809.
- [20] "GOES-R Series Data Book," 2019.
- [21] H. Schaub and J. L. Junkins, *Analytical Mechanics of Space Systems*. Reston, VA: AIAA Education Series, 4th ed., October 2019.
- [22] "Aerojet Rocketdyne propulsion helps enable new satellite servicing market," tech. rep., Aerojet Rocketdyne, 2020.
- [23] T. Marshall and M. Fletcher, "Meeting high-quality RWA commercial demand through innovative design," *Space Mechanisms and Tribology, Proceedings of the 8th European Symposium*, 1999.